The Holocene
http://hol.sagepub.com/

A sedimentary record of Holocene surface runoff events and earthquake activity from Lake Iseo (Southern Alps, Italy)

Stefan Lauterbach, Emmanuel Chapron, Achim Brauer, Matthias Hüls, Adrian Gilli, Fabien Arnaud, Andrea Piccin, Jérôme Nomade, Marc Desmet, Ulrich von Grafenstein and DecLakes Participants

The Holocene 2012 22: 749 originally published online 17 January 2012
DOI: 10.1177/0959683611430340

The online version of this article can be found at:
http://hol.sagepub.com/content/22/7/749

Published by:
SAGE
http://www.sagepublications.com

Additional services and information for *The Holocene* can be found at:

Email Alerts: http://hol.sagepub.com/cgi/alerts

Subscriptions: http://hol.sagepub.com/subscriptions

Reprints: http://www.sagepub.com/journalsReprints.nav

Permissions: http://www.sagepub.com/journalsPermissions.nav

Citations: http://hol.sagepub.com/content/22/7/749.refs.html

>> Version of Record - May 31, 2012

OnlineFirst Version of Record - Feb 16, 2012

OnlineFirst Version of Record - Jan 17, 2012

What is This?

Downloaded from hol.sagepub.com at ETH - Bibliothek on July 26, 2012

Research paper

A sedimentary record of Holocene surface runoff events and earthquake activity from Lake Iseo (Southern Alps, Italy)

The Holocene
22(7) 749–760
© The Author(s) 2012
Reprints and permission:
sagepub.co.uk/journalsPermissions.nav
DOI: 10.1177/0959683611430340
hol.sagepub.com
SAGE

Stefan Lauterbach,[1] Emmanuel Chapron,[2] Achim Brauer,[1] Matthias Hüls,[3] Adrian Gilli,[4] Fabien Arnaud,[5] Andrea Piccin,[6] Jérôme Nomade,[7] Marc Desmet,[8] Ulrich von Grafenstein[9] and DecLakes Participants[10]

Abstract

This study presents a record of Holocene surface runoff events and several large earthquakes, preserved in the sediments of pre-Alpine Lake Iseo, northern Italy. A combination of high-resolution seismic surveying, detailed sediment microfacies analysis, non-destructive core-scanning techniques and AMS ^{14}C dating of terrestrial macrofossils was used to detect and date these events. Based on this approach, our data shed light on past seismic activity in the vicinity of Lake Iseo and the influence of climate variability and human impact on allochthonous detrital matter flux into the lake. The 19 m long investigated sediment sequence of faintly layered lake marl contains frequent centimetre- to decimetre-scale sandy-silty detrital layers. During the early to mid Holocene, these small-scale detrital layers, reflecting sediment supply by extreme surface runoff events, reveal a distinct centennial-scale recurrence pattern. This is in accordance with regional lake-level highstands and minima in solar activity and thus apparently mainly climate-controlled. After *c.* 4200 cal. yr BP, intervals of high detrital flux occasionally also correlate with periods of enhanced human settlement activity. In consequence, deposition of small-scale detrital layers during the late Holocene apparently reflects a rather complex interplay between climatic and anthropogenic influences on catchment erosion processes. Besides the small-scale detrital layers, five up to 2.40 m thick large-scale detrital event layers, composed of basal mass-wasting deposits overlain by large-scale turbidites, were identified, which are supposed to be triggered by strong earthquakes. The uppermost large-scale event layer can be correlated to a documented M_w=6.0 earthquake in AD 1222 in Brescia. The four other large-scale event layers are supposed to correspond to previously undocumented local earthquakes. These occurred around 350 BC, 570 BC, 2540 BC and 6210 BC and most probably also reached magnitudes in the order of M_w = 5.0–6.5.

Keywords

climate, earthquakes, Holocene, Italy, lake sediments, land use, surface runoff events, Southern Alps

Received 9 September 2010; revised manuscript accepted 18 October 2011

Introduction

Damaging earthquakes as well as large floods, debris flows and surface runoff events constitute serious natural hazards to modern societies. The assessment of these hazards mainly relies on a thorough understanding of the particular recurrence patterns and underlying trigger mechanisms (natural and anthropogenic forcing). As such studies necessitate long continuous event records but historical data are mostly limited to only short periods (i.e. the past *c.* 500–1000 years), lake deposits provide ideal archives to study the recurrence of seismic activity and extreme hydrological events in the past. In consequence, several previous studies have successfully used lake sediments to establish long records of palaeoseismicity (e.g. Chapron et al., 1999; Migowski et al., 2004; Monecke et al., 2004; Nomade et al., 2005; Schnellmann et al., 2002; Strasser et al., 2006), river flooding (Arnaud et al., 2005; Bøe et al., 2006; Chapron et al., 2005; Debret et al., 2010; Moreno et al., 2008), debris flow activity (Dapples et al., 2002; Irmler et al., 2006) and extreme surface runoff events (Mangili et al., 2005).

Owing to its high population density and importance for national economy, central-northern Italy is particularly vulnerable to the effects of these natural hazards. However, until now, regional lake sediment records have only rarely been utilized to reconstruct past earthquake activity (e.g. Fanetti et al., 2008). Furthermore, while several studies in the northwestern Alps addressed hydrological changes during the Holocene (e.g.

[1]GFZ German Research Centre for Geosciences, Germany
[2]ISTO CNRS-Université d'Orléans, France
[3]Christian-Albrechts-University, Germany
[4]Swiss Federal Institute of Technology (ETH) Zurich, Switzerland
[5]EDYTEM CNRS-Université de Savoie, France
[6]Regione Lombardia, Direzione Generale Territorio e Urbanistica, Struttura Sistema Informativo Territoriale, Italy
[7]ISTerre CNRS-Université Joseph Fourier, France
[8]ISTO CNRS-Université François Rabelais de Tours, France
[9]CEA CNRS-Laboratoire des Sciences du Climat et de l'Environnement, France
[10]Soumaya Belmecheri (LSCE, Gif-sur-Yvette), Nils Andersen, Helmut Erlenkeuser (Leibniz Laboratory, Kiel), Ángel Baltanás, (Universidad Autónoma, Madrid), Dan L. Danielopol (Institute for Limnology, Mondsee), Georg Hoffmann (LSCE, Gif-sur-Yvette), Christian Wolff (GFZ, Potsdam)

Corresponding author:
Stefan Lauterbach, GFZ German Research Centre for Geosciences, Section 5.2 – Climate Dynamics and Landscape Evolution, Telegrafenberg, 14473 Potsdam, Germany.
Email: slauter@gfz-potsdam.de

Downloaded from hol.sagepub.com at ETH - Bibliothek on July 26, 2012

Magny, 1993a, b, 2004; Magny et al., 2010), regional data on palaeohydrological changes for northern and central Italy are still sparse (e.g. Magny et al., 2007, 2009a). This is of particular interest as changes in the hydrological cycle might have influenced the recurrence of floods, landslides and surface runoff events in the region and in addition also affected pre-historic societies (Arbogast et al., 2006; Magny, 2004). Within this context, also the influence of anthropogenic settlement activity on precipitation-triggered catchment erosion is still matter of debate (Dapples et al., 2002; Irmler et al., 2006; Schneider et al., 2010).

As part of the European Science Foundation project DecLakes (*Decadal Holocene and Lateglacial variability of the oxygen isotopic composition in precipitation over Europe reconstructed from deep-lake sediments*), this study introduces the sedimentary record of pre-Alpine Lake Iseo in northern Italy. A combined seismic and sedimentological approach is used to identify exceptional depositional events, namely large- and small-scale turbidites and mass-wasting deposits, in a sediment core from the Sale Marasino Basin, a subbasin of Lake Iseo. Based on a core chronology established through AMS ^{14}C dating of terrestrial macrofossils, this allows (1) the reconstruction of local surface runoff activity, influenced by both climate variability and human impact in the surrounding area, and (2) the identification of several major regional earthquakes during the Holocene.

Study site and tectonic setting

Lake Iseo (Latin name Sebino) is the fourth largest lake in northern Italy (surface area ~60.9 km²). It is located at the southern end of the Camonica Valley in the foothill zone of the Lombardian Southern Alps at 185 m a.s.l., about 20 km northwest of Brescia (Figure 1a and b). According to Bini et al. (1978), the present lake basin, which in its northern and central part is surrounded by 1000–1400 m high mountain ranges (Garibaldi et al., 1999), is the result of Pleistocene glacier activity, reshaping a pre-existent late Miocene erosional canyon. The catchment area of Lake Iseo (~1842 km²), which has a mean altitude of ~1400 m (Garibaldi et al., 1999), extends only several kilometres to the south, east and west of the lake, but stretches up to 60 kilometres northwards into the Camonica Valley. In its northern part the surrounding mountain ranges reach altitudes between 2000 and more than 3500 m in the Adamello Massif. The valley and thus the catchment of Lake Iseo are drained by the Oglio River and its tributaries, the former being, besides some minor streams and the Borlezza River in the northwest, the main inflow and only outflow of Lake Iseo (Garibaldi et al., 1999). Monte Isola Island in the central part of the lake is one of the largest lake islands in Europe (surface area ~4 km², peak elevation ~420 m above lake level).

The earliest documented traces of human presence in the Lake Iseo region, namely rock carvings in the Camonica Valley, date to the Mesolithic (Anati, 1994) and there is pollen evidence for the onset of first but sparse agricultural activity during the early Neolithic (around 7000 cal. yr BP) and continuous anthropogenic land use in the area since then (for a detailed account see Gehrig, 1997).

The present climate in the region is humid subtropical with mean annual air temperatures of 12.7°C and January and July means of about 2.0°C and 23.1°C, respectively (all temperature data for Bergamo/Orio al Serio for the period 1981–1990, Vose et al., 1992). The local precipitation regime is characterized by two not very pronounced maxima in late spring and autumn and an annual average of ~1200 mm.

The combination of multibeam bathymetry (EM3000) and laser scan survey (LIDAR) data from a previous study on the geomorphology of the Lake Iseo basin (Bini et al., 2007) with a

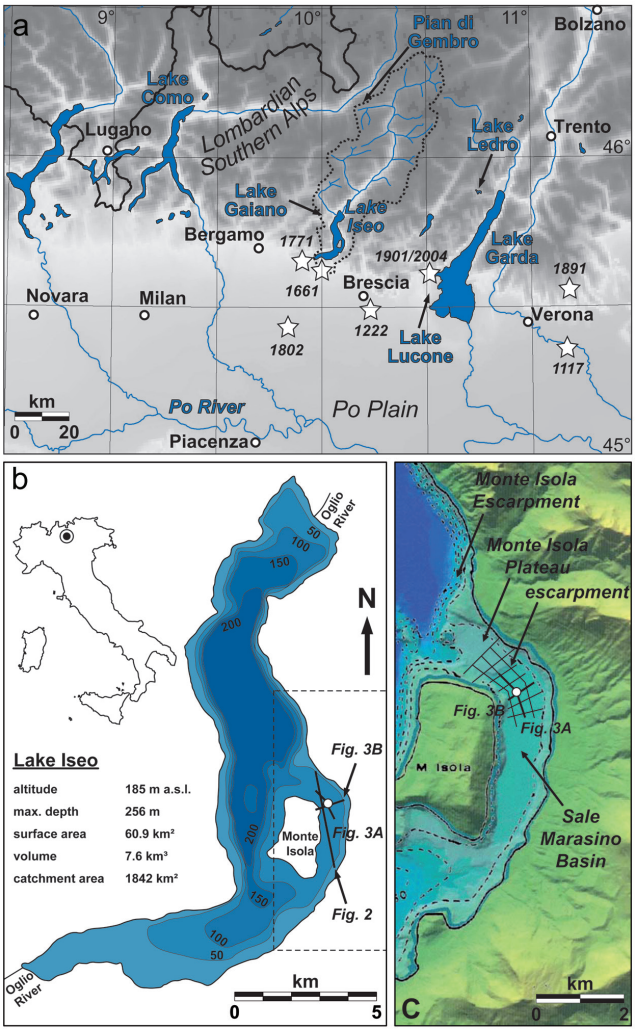

Figure 1. (a) General geographic overview map of central-northern Italy with Lake Iseo and other locations mentioned in the text. Stars denote the locations of major regional earthquakes given in Table 1. The dashed line indicates the catchment area of Lake Iseo. (b) Simplified bathymetric map of Lake Iseo with the coring site (white point) and the location of the seismic profiles presented in Figures 2 and 3. All depths are given in metres below lake level. (c) Detailed geomorphology of the eastern subbasin of Lake Iseo as reflected by multibeam bathymetry and laser scan data included into a regional digital elevation model. Acquisition of the 3.5 kHz seismic profiles (black lines) focused on the Monte Isola Plateau and the northern part of the Sale Marasino Basin in order to precise the stratigraphy at the coring site (white point)

digital elevation model (Figure 1c) allows to illustrate the main morphological features of the area surrounding the eastern subbasin of Lake Iseo between Monte Isola Island and the eastern lake shore. This subbasin, which is at its northern margin separated from the deep central basin (maximum water depth ~256 m) by the submerged Monte Isola Escarpment (Bini et al., 2007), can be divided into a shallower northern (Monte Isola Plateau (MIP), water depth ~79 m) and a deeper southern part (Sale Marasino Basin (SMB), water depth ~100 m), where the coring site is located. Both parts are separated by a small, NE–SW trending escarpment of about 20 m height. While the western margin of the SMB is characterized by the steep slopes of Monte Isola Island, the eastern more gently sloped flank reveals numerous gullies and canyons as well as subaquatic detrital fans (Bini et al., 2007). Triassic to Jurassic dolomites and limestones together with Plio-Pleistocene fluvial and glacial deposits represent the main geological units exposed along the

Downloaded from hol.sagepub.com at ETH - Bibliothek on July 26, 2012

Table 1. Major earthquakes during the past *c.* 900 years in the vicinity of Lake Iseo. All data are given according to Italian earthquake catalogues (CPTI Working Group, 2004; Guidoboni et al., 2007)

Year	Location	Distance from Lake Iseo	Moment magnitude M_w	Epicentral intensity I_0
AD 2004[a]	Salò	~35 km southeast	5.0	VII–VIII
AD 1901[a]	Salò	~35 km southeast	5.7	VIII
AD 1891	Valle d'Illasi	~90 km southeast	5.7	VIII–IX
AD 1802	Soncino	~40 km southwest	5.7	VIII
AD 1771	Sarnico	southern lake shore	4.8	VI
AD 1661	Montecchio	southern lake shore	5.2	VII
AD 1222	Brescia	~25 km southeast	6.0	VIII–IX
AD 1117	Verona	~75 km southeast	6.5	IX–X

[a] Instrumentally recorded.

shorelines in the vicinity of the coring site (Bini et al., 2007; Cassinis et al., 2009).

The regional tectonic setting of central-northern Italy, particularly the formation of a fold-and-thrust belt since the late Oligocene, is the result of the post-collisional phase of the Alpine orogeny (e.g. Dal Piaz et al., 2003 and references therein). Although crustal shortening in the Lombardian Southern Alps has previously been assumed to slow or even cease during the late Miocene (Castellarin et al., 2006; Fantoni et al., 2004), recent geomorphological studies revealed that the complete thrust front was tectonically active throughout the Plio-Pleistocene (Burrato et al., 2003; Chunga et al., 2007; Livio et al., 2009; Sileo et al., 2007). The crustal shortening, which still proceeds with rates of ~1.1 mm/yr in the Lake Iseo area (Serpelloni et al., 2005), is mainly accommodated by blind thrusts and fault-propagation folding of Pleistocene strata (Livio et al., 2009; Sileo et al., 2007), reflected by a few regional historical earthquakes with moment magnitudes of $M_w \geq 5.0$ and epicentral intensities of $I_0 \geq$ VII (Table 1; Boschi et al., 2000; CPTI Working Group, 2004; Guidoboni et al., 2007). In general, seismic activity in the Lake Iseo area is mainly confined to an arcuate zone extending about 30–40 km to the south and southeast of the lake (CPTI Working Group, 2004; Guidoboni et al., 2007). This zone comprises the WSW–ENE trending Val Trompia fold-and-thrust belt and its continuation in the Lake Garda region, the SSW–NNE trending Giudicarie Fault System (Castellarin and Cantelli, 2000; Fantoni et al., 2004; Livio et al., 2009).

Fieldwork and methods

Seismic reflection surveys

During the first seismic reflection survey on Lake Iseo in 2002, which was carried out with a broad-band (300–2400 kHz) single-channel boomer device (Bini et al., 2007), only one axial profile was acquired across the eastern subbasin (Figure 2). This profile was used to select a suitable location for the coring site

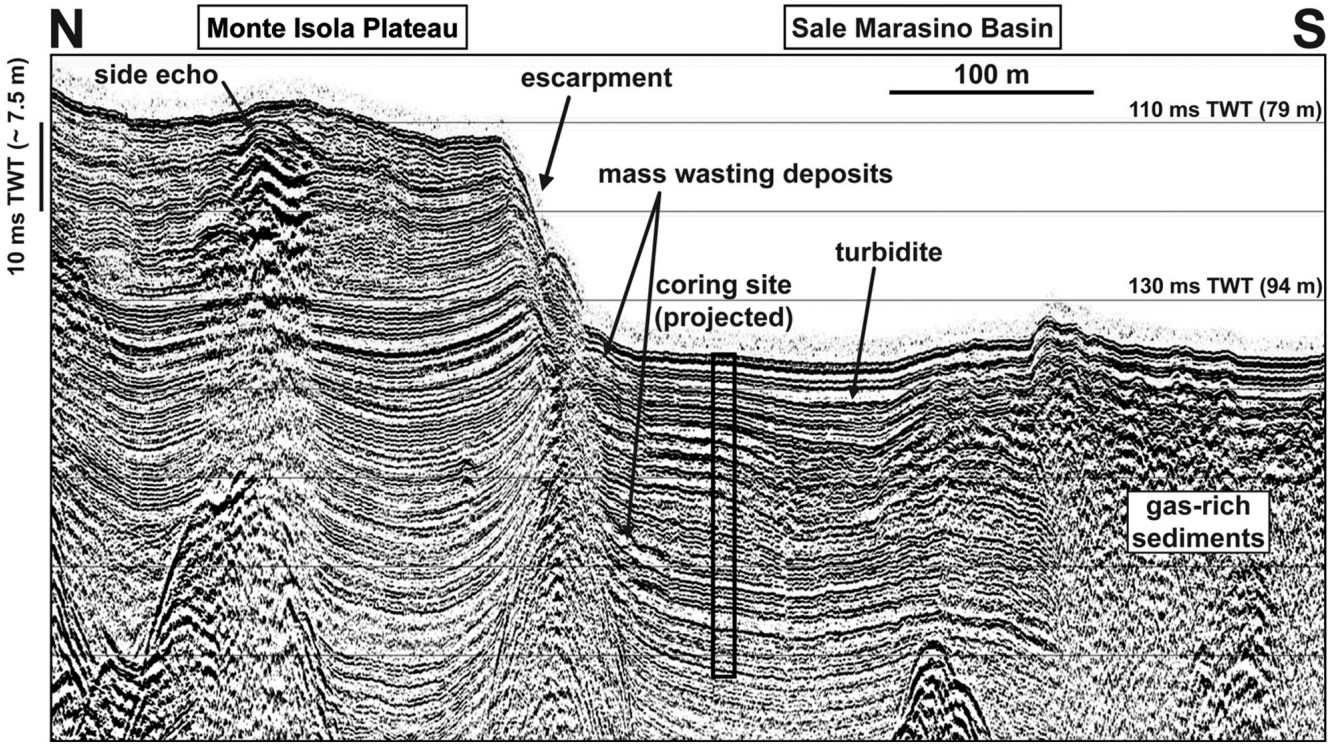

Figure 2. High-resolution seismic profile (boomer) across the eastern subbasin of Lake Iseo, illustrating the main sedimentary environments that characterize this part of the lake and have previously been documented by Bini et al. (2007). This seismic profile (see Figure 1) was used to select the coring site. The frequent occurrence of mass-wasting deposits and the identification of a large-scale turbidite deposit in the Sale Marasino Basin suggest that subaquatic landslides essentially originate from the escarpment that separates the basin from the Monte Isola Plateau

Downloaded from hol.sagepub.com at ETH - Bibliothek on July 26, 2012

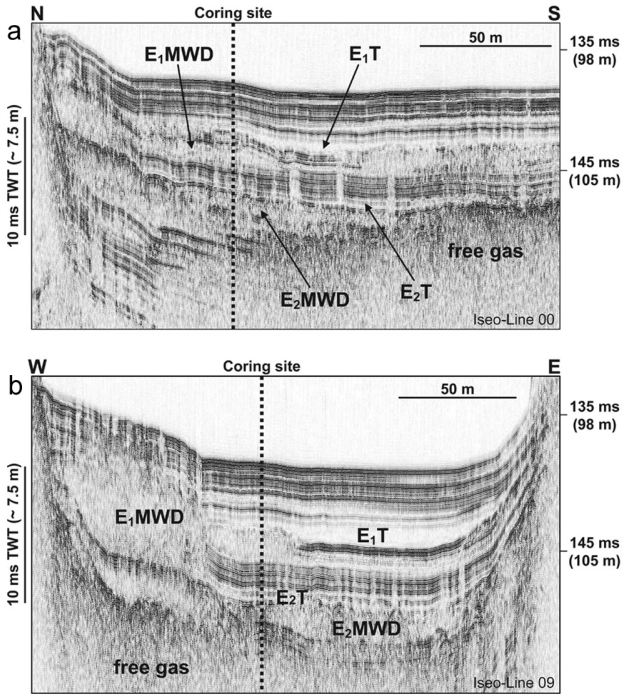

Figure 3. Two high-resolution seismic profiles (3.5 kHz), acquired in N–S (a) and E–W (b) direction and intersecting close to the coring location, illustrate the basin infill geometry of the northern Sale Marasino Basin. The occurrence of free gas in the sediments, which limits acoustic imaging below about 7 m sediment depth, is indicated together with the large-scale mass-wasting (E_1MWD and E_2MWD) and turbidite deposits (E_1T and E_2T) discussed in the text

(45°43'07"N, 10°06'12"E), which is located at about 100 m water depth, close to the deepest part of the SMB (Figure 1b and c), within an area of relatively well-stratified sediments.

In 2007, a new high-resolution seismic reflection survey was performed across the MIP and the SMB by using the 3.5 kHz pinger device and Octopus acquisition system of the ETH Zurich, mounted on an inflatable boat. A dense grid of seismic profiles was acquired, precisely imaging the stratigraphy of the sedimentary basin infill at the coring site (Figure 3a and b). Seismic data processing (band-pass filtering) and interpretation were performed at the University of Orléans by using the programs SeiSee and KINGDOM Suite, respectively.

Coring

Three parallel sediment cores (SEB 05_02, SEB 06_03 and SEB 06_04), each consisting of 2 m long segments, were recovered from the coring site during the field campaigns in 2005 and 2006 by using a 90 mm diameter UWITEC piston corer. Additionally, three short gravity cores (SEB 05_02P1, SEB 06_03P1 and SEB 06_03P2) were retrieved in order to obtain the undisturbed sediment–water interface. All core segments were already split into halves, lithostratigraphically described, photographed and subsampled on-site in a field lab. The segments of the three long sediment cores and gravity core SEB 06_03P2 were visually correlated by using more than 80 macroscopically visible lithological marker layers, resulting in an about 19 m long continuous composite profile (Figure 4a). Owing to core loss and the lack of overlapping segments in the parallel cores, the two lowermost segments of core SEB 06_03 could not be linked to the continuous composite profile and thus remain floating (Figures 4 and 5) with their position given according to the intended depth in the coring protocol.

Sediment properties and dating

Continuous measurements of diffuse spectral reflectance of all core segments at 1 cm intervals were carried out prior to subsampling in the field lab with a Minolta CM-2500d spectrophotometer (0.8 mm spot size). For the measurements, the fresh sediment surface was covered with a thin transparent polyethylene film (Chapman and Shackleton, 1998). The mean reflectance intensity, measured at 10 nm increments over the 400–700 nm wavelength range, results in the sediment lightness L*, given on a scale from 0 (black) to 100 (white).

For detailed sediment microfacies analysis, which was carried out at the GFZ in Potsdam, a set of large-scale petrographic thin sections was prepared from overlapping sediment blocks (100 mm × 20 mm ×10 mm), taken continuously from all cores of the composite profile, following the method described by Brauer et al. (1999) and Brauer and Casanova (2001). Thin sections were examined under a ZEISS Axiophot polarization microscope at 25–400× magnification.

Magnetic susceptibility measurements were conducted on split cores at 0.5 cm steps with a Bartington MS2E point sensor mounted on a GEOTEK multisensor core logger at the University of Franche-Comté in Besançon. The results are expressed as SI units.

For establishing a chronology for the Lake Iseo sediment sequence, 29 samples of terrestrial plant macrofossils (wood, small twigs, seeds, leaf fragments) were selected from the cores of the composite profile (Table 2) and AMS ^{14}C-dated at the Leibniz Laboratory in Kiel. Conventional radiocarbon ages were calibrated using the OxCal 4.1 program (Ramsey, 1995, 2001) with the IntCal09 calibration data set (Reimer et al., 2009). All calibrated ages are reported as 2σ probability ranges.

Results

Seismic stratigraphy

On the boomer profile, the northern part of the SMB is characterized by a well-stratified acoustic facies, reaching more than 40 ms two-way-travel time (TWT) in thickness (Figure 2). In contrast, the very limited acoustic penetration of only 5 ms TWT in the southern SMB suggests the local occurrence of free gas in the sedimentary basin infill. South of the coring site, a large turbidite deposit, characterized by a transparent acoustic facies and laterally developing onlaps, is identified at 140 ms TWT. At the edge of the escarpment that separates the SMB and the MIP, several lense-shaped bodies with a transparent to chaotic acoustic facies indicate local mass-wasting deposits that may have reworked sediments at the coring site. On the MIP, acoustic penetration locally reaches about 70 ms TWT. Several small-scale lense-shaped bodies with a chaotic acoustic facies, which are found within the upper 20 ms TWT, indicate recurrent but spatially limited subaquatic mass-wasting events.

Acoustic penetration of the pinger profiles in the SMB is limited to 10–15 ms TWT below the lake floor, suggesting free gas in the sediments below (Figure 3a and b). Within the upper acoustic level, which reveals well-stratified and parallel continuous reflections, several intercalated large-scale mass-wasting deposits can be identified. The uppermost transparent layer, which is interpreted as a large-scale turbidite (E_1T), is characterized by a high-amplitude basal reflection and develops lateral onlaps along the eastern, western and northern edges of the basin. This layer caps a lense-shaped mass-wasting deposit (E_1MWD) with a chaotic to transparent acoustic facies and irregular basal and upper boundaries, which reaches its maximum thickness near the base of the escarpment and thins towards the southeast. A second transparent layer, which is also considered as a large-scale turbidite (E_2T), reaches its maximum thickness in the deepest part of the basin and also develops onlaps at the basin edges. It locally drapes another lense-shaped mass-wasting deposit (E_2MWD), which is characterized by a chaotic to transparent acoustic facies and an

Downloaded from hol.sagepub.com at ETH - Bibliothek on July 26, 2012

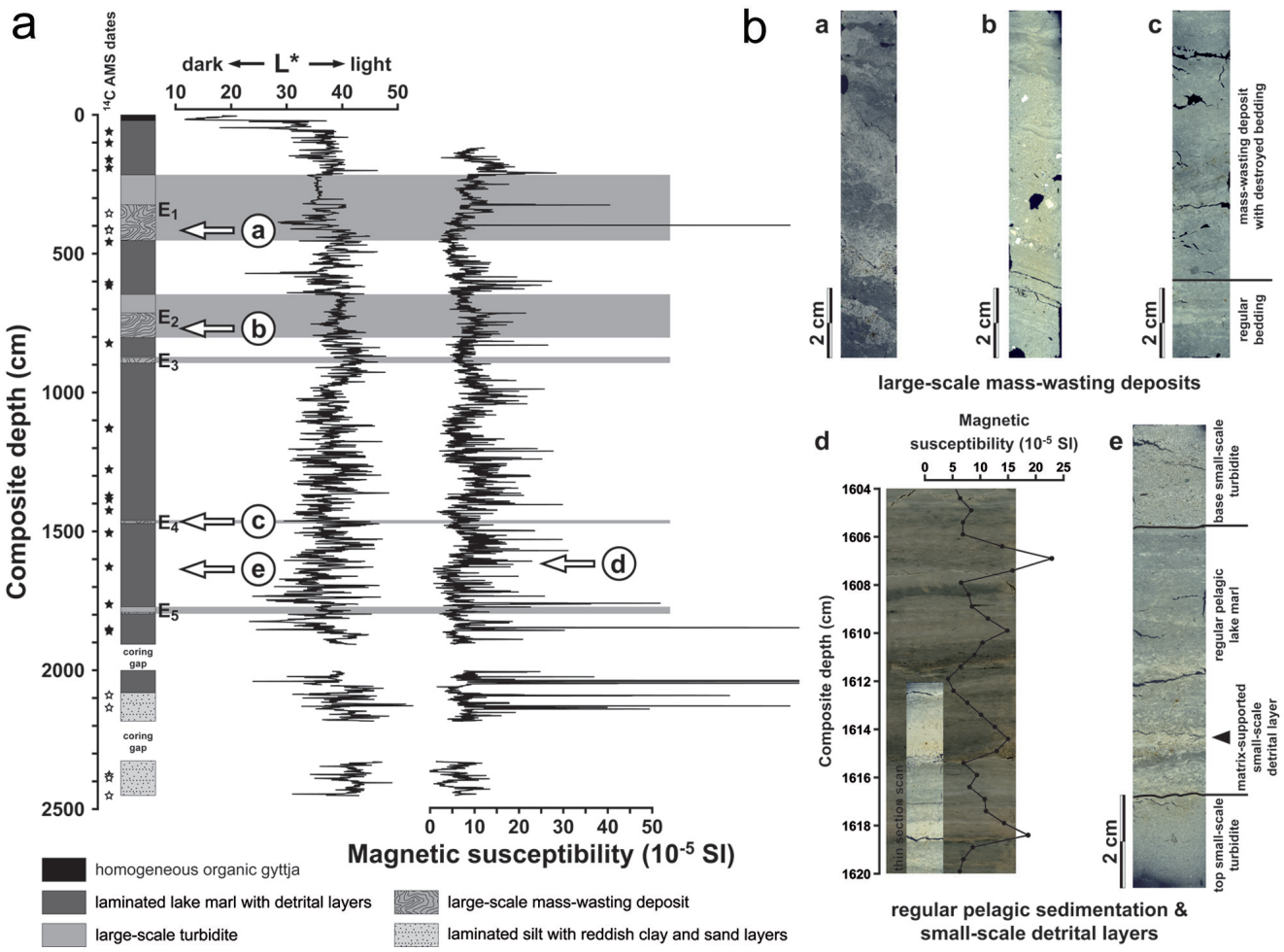

Figure 4. (a) Results of diffuse spectral reflectance (sediment lightness L*) and magnetic susceptibility measurements on the Lake Iseo sediment record. Stars indicate AMS ^{14}C dates (black: included in the age–depth model; white: excluded). Grey horizontal bars indicate the position of the earthquake-induced large-scale event layers E_1 to E_5. Arrows indicate the position of sediment microfacies structures presented in (b). (b) Sediment microfacies of large-scale mass-wasting deposits, regular pelagic sediments and small-scale detrital layers as revealed from large-scale petrographic thin sections (pictures a–e) and core photographs (picture d). Large-scale mass-wasting deposits are characterized by destroyed layering and liquefaction structures (pictures a and c) and chaotic sediment sequences with randomly dispersed up to gravel-sized intraclasts (picture b). The regular pelagic lake marl is intercalated by frequent small-scale turbidites and matrix-supported detrital layers (pictures d and e), which are well reflected by peaks in magnetic susceptibility (picture d)

irregular upper boundary, but also several chaotic internal high-amplitude reflections that locally absorb the acoustic signal. This mass-wasting deposit seems to be thicker at the foot of the escarpment and extends over the complete width of the SMB.

Sediment microfacies and proxy data

Regular pelagic sedimentation and small-scale detrital layers. The sediment record of Lake Iseo can be subdivided into three major lithostratigraphical units. The uppermost 21.0 cm of the sediment profile consist of a black organic gyttja and are characterized by a sediment lightness L* smaller than ~20. This unit is supposed to represent deposition during the recent phase of eutrophication, i.e. approximately the past five to six decades.

The second unit, comprising the largest part of the sediment record (21.0–2078.0 cm), is composed of light to brownish grey, partly blackish, silt- to clay-sized pelagic lake marl that displays a faint centimetre-scale layering. Major constituents are microcrystalline endogenic calcite, clay minerals, finely dispersed detrital carbonates and siliciclastics (up to 100 µm in diameter), amorphous organic matter, diatom frustules and ostracod valves. Locally, a faint millimetre-scale lamination of light, carbonate-rich layers and dark layers, containing clay minerals, amorphous organic matter and diatom frustules, is observed. However, the macroscopic layering is mainly owed to the lithological contrast between the autochthonous lake marl and frequently intercalated, brownish grey sand/silt layers. These small-scale detrital layers are mainly composed of angular allochthonous carbonates and siliciclastics (feldspar, quartz and mica) between 50 and 500 µm in diameter, but often also contain terrestrial plant material (e.g. wood, leaves, seeds, fruits), charcoal particles and fragments of gastropods and bivalves. In general, two types of small-scale detrital layers can be distinguished. Distinct detrital layers (0.5–18.5 cm thick) reveal a clear upward gradation from sand/silt to clay (Figure 4b, picture e) and sharp, occasionally erosional, basal contacts. Matrix-supported detrital layers are thinner than graded layers (<0.5 cm) and show no gradation. As the coarse-grained minerogenic detritus is finely dispersed within the lake marl, only indistinct layer boundaries are observed. The small-scale detrital layers are reflected by distinct fluctuations in sediment lightness towards lighter (L*>40, high content of detrital carbonates) or darker (L*<35, abundant organic material) colour and by peaks in magnetic susceptibility (Figure 4a and b, picture d). The latter is attributed to the concentration of allochthonous magnetic minerals (Thompson et al., 1975) and larger grain sizes (Bradshaw and Thompson, 1985) in these layers.

Sediments of the third lithostratigraphical unit occur only in the two lowermost floating core segments below 2078.0 cm composite depth. These deposits reveal a distinct centimetre-scale lamination of light grey silt layers and frequently intercalated brownish to reddish clay and sand layers.

Downloaded from hol.sagepub.com at ETH - Bibliothek on July 26, 2012

Table 2. AMS ^{14}C dates obtained from terrestrial macrofossils from Lake Iseo. All conventional radiocarbon dates were calibrated using OxCal 4.1 (Ramsey, 1995, 2001) with the IntCal09 calibration data set (Reimer et al., 2009). Italicised samples were not considered for the age–depth model (for explanations see the results section)

Sample/Lab. code	Composite depth (cm)	Dated material	Carbon content (mg) / δ^{13}C (‰)	AMS ^{14}C age (yr BP ± 1σ)	Calibrated age (cal. yr BP, 2σ range)
KIA39233	59.50	twig	1.34 / –26.94 ± 0.49	134 ± 25	9–275[a]
KIA39234	101.00	twig	5.85 / –27.79 ± 0.27	209 ± 27	–4–303[a]
KIA39235	159.50	wood & leaf fragments[b]	1.56 / –23.80 ± 0.13	677 ± 29	561–679
KIA39236	190.00	twigs	2.38 / –26.24 ± 0.34	672 ± 26	561–675
KIA33098	*354.00*	*wood*	*4.27 / –25.79 ± 0.11*	*1370 ± 22*	*1269–1316*
KIA29385	*412.00*	*olive seed*	*4.60 / –28.04 ± 0.08*	*1225 ± 24*	*1068–1257*
KIA29388	*414.00*	*plant remains[b]*	*4.57 / –25.30 ± 0.11*	*1256 ± 25*	*1091–1277*
KIA33099	457.00	wood & twig	5.33 / –26.53 ± 0.10	1296 ± 24	1178–1287
KIA36621	606.00	plant remains[b]	5.40 / –27.29 ± 0.50	2201 ± 32	2135–2327
KIA33100	614.25	wood	4.38 / –26.34 ± 0.09	2232 ± 24	2155–2335
KIA36622	822.00	plant remains[b]	2.30 / –27.40 ± 0.38	2434 ± 27	2354–2699
KIA29390	1127.00	plant remains[a]	1.87 / –27.62 ± 0.20	3016 ± 27	3081–3335
KIA29386	1128.25	wood	3.92 / –28.40 ± 0.57	3018 ± 25	3082–3335
KIA33109	1276.00	beech nut	4.28 / –27.62 ± 0.11	3319 ± 29	3473–3631
KIA33101	1372.75	wood	2.48 / –25.87 ± 0.09	3728 ± 26	3985–4151
KIA33102	1383.50	twig	4.62 / –29.81 ± 0.16	3803 ± 25	4090–4286
KIA33103	1423.00	shell of beech nut	4.67 / –27.59 ± 0.36	3854 ± 33	4155–4411
KIA29387	1503.25	wood	2.98 / –27.47 ± 0.15	4206 ± 29	4628–4846
KIA33110	1503.75	twigs & wood	1.91 / –28.68 ± 0.16	4240 ± 28	4655–4859
KIA29392	1626.00	plant remains[b]	1.84 / –28.11 ± 0.12	5484 ± 36	6207–6394
KIA33104	1762.00	wood	4.82 / -28.90 ± 0.19	7124 ± 36	7866–8014
KIA33112	1851.50	wood & leaf	3.53 / –24.95 ± 0.08	8382 ± 35	9302–9484
KIA33105	1852.50	wood	0.92 / –29.50 ± 0.11	8296 ± 52	9129–9444
KIA33106	1857.50	wood & plant remains[b]	3.01 / –29.37 ± 0.14	8369 ± 37	9297–9476
KIA33107	*2088.00*	*twig*	*3.34 / –25.31 ± 0.09*	*11,931 ± 47*	*13,636–13,940*
KIA33108	*2134.00*	*wood & leaves*	*3.97 / –26.13 ± 0.13*	*12,470 ± 49*	*14,175–15,024*
KIA39237	*2376.00*	*wood & bark*	*4.84 / –27.91 ± 0.40*	*13,225 ± 54*	*15,475–16,680*
KIA39238	*2386.00*	*twig*	*5.20 / –25.45 ± 0.34*	*13,232 ± 65*	*15,463–16,700*
KIA30286	*2449.00*	*plant remains[b]*	*0.73 / –28.87 ± 0.22*	*14,950 ± 126*	*17,859–18,567*

[a]This sample falls within a ^{14}C plateau caused by an increase in solar activity (Maunder minimum) and fossil fuel burning (Suess effect). It is thus only possible to determine a comparatively large calibration range.
[b]Various undetermined terrestrial plant remains (leaves, wood, seeds).

Large-scale event layers. Within the sediments of the second lithostratigraphical unit, five large-scale event layers occur, which exhibit a characteristic sedimentological bipartition. The uppermost event layer E_1 (216.0–452.0 cm) reveals a 128.3 cm thick basal sequence of similar composition as the regular pelagic lake marl. However, the macroscopic sediment appearance is wet and unconsolidated and microfacies analysis reveals a largely destroyed and indistinct layering, extensive sediment homogenization and occasional liquefaction structures (Figure 4b, picture a). This sequence can be correlated to the upper large-scale mass-wasting deposit E_1MWD in the seismic stratigraphy. It is overlain by a 107.7 cm thick graded layer with a distinct, about 10 cm thick sandy base with abundant organic macro remains, rapidly fining upwards into silt and clay. This layer is interpreted as a large-scale turbidite, corresponding to event layer E_1T in the seismic stratigraphy. While the signature of the basal mass-wasting deposit in the core-scanning data is ambiguous owing to the partly preserved primary sediment structure, the overlying, rather homogeneous turbidite is clearly visible through almost constant sediment lightness (Figure 4a).

Event layer E_2 (646.1–802.0 cm) contains a 89.0 cm thick basal part, which is characterized by a chaotic sequence of (1) autochthonous pelagic lake marl with destroyed and tilted layering, (2) small-scale graded sand/silt layers and lenses (up to 8.5 cm thick) and (3) homogenized, clay-sized autochthonous sediment with randomly dispersed gravel-sized dolomitic and siliciclastic intraclasts and lumps of finely-laminated lake marl (Figure 4b, picture b). This sequence, which can be correlated to the lower large-scale mass-wasting deposit E_2MWD in the seismic stratigraphy, is overlain by a 66.9 cm thick graded layer that exhibits a distinct upward fining from coarse sand to clay. This corresponds to the large-scale turbidite E_2T in the seismic stratigraphy. Relatively constant sediment lightness clearly reflects extensive sediment homogenization throughout the entire event layer E_2 (Figure 4a). Strong fluctuations and high peaks (up to 20 $\times 10^{-5}$ SI units) in magnetic susceptibility within the basal mass-wasting deposit reflect the finely dispersed sand- and gravel-sized carbonate detritus, while rather constant values within the overlying turbidite mirror extensive sediment homogenization and upward-fining.

Besides the two exceptionally thick event layers E_1 and E_2, three other large-scale event layers with a similar sedimentological bipartition are found in the lower part of the sediment profile. However, owing to their limited thickness and to the occurrence of free gas in the deeper sediments, these layers are not seen in the seismic profiles. Event layer E_3 (871.1–893.5 cm) contains a 17.8 cm thick basal mass-wasting deposit of macroscopically wet and homogeneous appearance, which is characterized by destroyed and folded layering and overlain by a 4.6 cm thick turbidite. The 7.9 cm thick basal mass-wasting deposit of event layer E_4 (1458.7–1470.5 cm) also exhibits destroyed layering (Figure 4b, picture c) and is capped by a 3.9 cm thick turbidite. Event layer E_5 (1771.0–1796.0 cm) contains a 5.5 cm thick basal mass-wasting deposit with destroyed and folded layering, which is overlain by a 19.5 cm thick sequence of three separate turbidites.

Downloaded from hol.sagepub.com at ETH - Bibliothek on July 26, 2012

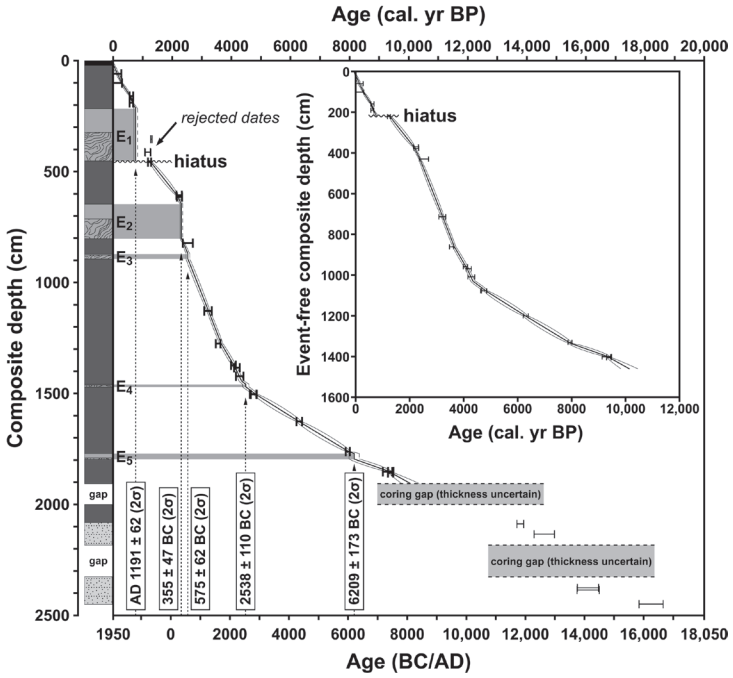

Figure 5. Age–depth model for the Lake Iseo sediment record derived from AMS ^{14}C dating of terrestrial macrofossils (Table 2). Error bars for individual radiocarbon dates indicate calibrated 2σ ranges (bold: included in the age–depth model; thin: excluded). The bold line between individual radiocarbon dates represents the age–depth model derived from the *P_Sequence* deposition model (*k*=0.5) implemented in the OxCal 4.1 program (Ramsey, 2008). Dashed lines represent the 2σ probability range of the age–depth model. The inset figure illustrates the age–depth model corrected for large-scale event layers. Grey horizontal bars indicate the position of earthquake-induced large-scale event layers E_1 to E_5, given with the corresponding ages in years BC/AD

Chronology

All 29 terrestrial macrofossil samples obtained for AMS radiocarbon dating (24 samples from the continuous upper ~19 m of the profile and 5 samples from the two floating basal core segments) were derived from detrital layers and thus might tend to give too old calibrated ages because of sample material reworking. However, several cross-datings on wood, which is prone to reworking, and other presumably less affected terrestrial macro remains (leaf fragments, seeds, etc.) obtained from the same or adjacent event layers (KIA33112/KIA33105/KIA33106, KIA29387/KIA33110, KIA29390/KIA29386, KIA36621/KIA33100, KIA29385/KIA29388) reveal consistent calibrated ages with overlapping 2σ ranges. It is thus inferred that reworking of wood samples should be negligible.

The Bayesian-based *P_Sequence* deposition model with the parameter *k*=0.5 (depositional events per unit length), implemented in the OxCal 4.1 program (Ramsey, 2008), was used for generating an age–depth model for the continuous upper ~19 m of the sediment record (Figure 5). Out of the 24 dated samples from this interval, three samples (KIA33098, KIA29385 and KIA29388) were rejected for modelling as they were obtained from large-scale event layer E_1 and thus do not belong to an in situ sediment sequence. The remaining 21 calibrated ages and an age of −56 cal. yr BP for the sediment–water interface (coring campaign in spring 2006) were used as input parameters for age–depth modelling. As the large-scale event layers correspond to instantaneous ('time-neutral') depositional events, the final age–depth model was calculated based on a corrected composite depth with the thickness of these event layers being subtracted (inset of Figure 5). The final age–depth model yielded a model agreement index A_{model} of 72.5%, which is fairly above the threshold of 60% (Ramsey, 1995, 2008). Although also small-scale graded and matrix-supported detrital layers represent instantaneous depositional events, these were not removed from the final age–depth model, because their reflection in the magnetic susceptibility record enables investigating their recurrence pattern throughout the record. An alternative age–depth model, where all small-scale graded detrital layers thicker than 1.5 cm were removed reveals, however, only negligible deviations from the original age–depth model. These in general do not exceed the 2σ confidence interval (i.e. 100–200 years) between individual radiocarbon dated samples, thus supporting our approach.

The continuous upper ~19 m of the Lake Iseo sediment record cover approximately the past 10,000 years (Figure 5). As revealed from the modelled age of 759±62 cal. yr BP for the top of large-scale event layer E_1 and a radiocarbon date of 1233±54 cal. yr BP obtained from a macrofossil sample (KIA33099) 5 cm below this event, we suggest an erosional hiatus of *c.* 500 years (equivalent to about 1 m of sediment) below event layer E_1. Owing to their floating stratigraphical position, no age model was constructed for the two lowermost core segments of the profile. However, radiocarbon dates of 15,463–16,700 and 17,859–18,567 cal. yr BP (KIA39238 and KIA30286; Table 2) from the top and the base of the lowermost core segment, respectively, indicate that post-glacial lacustrine sediments in the SMB have an age of at least *c.* 18,000 cal. yr BP (the base of the lacustrine deposits was not recovered). Presuming that the dated material is not reworked, this in turn yields an older minimum age for the retreat of the last glacial maximum glacier from the lake basin than the previous estimate of >16,000 cal. yr BP (Bini et al., 2007).

Sedimentation rates (Figure 6) for both the original and the alternative age–depth model are lowest (~0.5–1.0 mm/yr) between *c.* 10,000 and 4300 cal. yr BP, then increase to ~2.5–3.0 mm/yr from *c.* 4300 to 3700 cal. yr BP and reach highest levels of ~3.0–3.5 mm/yr from *c.* 3700 to 2400 cal. yr BP. This period is followed by slightly decreasing values of ~2.4–2.7 mm/yr between *c.* 2400 and 2200 cal. yr BP and a subsequent drop to relatively low levels of ~1.7 mm/yr from *c.* 2200 to 1300 cal. yr BP. Another period of high sedimentation rates (~2.6–3.5 mm/yr) occurs between *c.* 1300 and 600 cal. yr BP. After another short drop to ~2.0 mm/yr between *c.* 600 and 300 cal. yr BP, sedimentation rates rise again to ~2.7–3.1 mm/yr during the last *c.* 350 years (all values excluding the large-scale event layers and the *c.* 500 year long hiatus). Modelled ages for the two large event layers E_1

Downloaded from hol.sagepub.com at ETH - Bibliothek on July 26, 2012

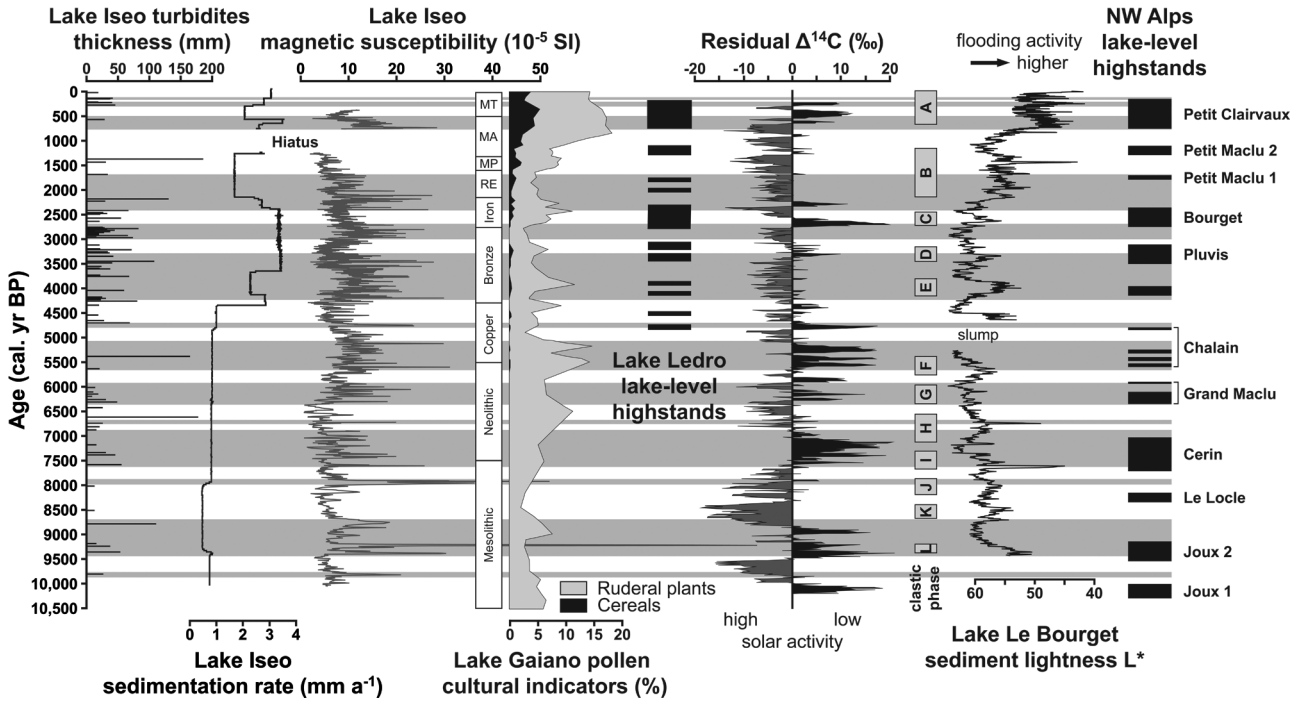

Figure 6. Comparison of Lake Iseo sedimentation rate and proxy records for detrital matter flux (distinct small-scale turbidites of >1.5 cm thickness, magnetic susceptibility) with cultural stages in central-northern Italy (RE: Roman Empire; MP: Migration Period; MA: Middle Ages; MT: Modern Times) and indicators for agricultural activity in the Lake Gaiano pollen record (modified after Gehrig, 1997), lake-level highstands in Lake Ledro (Magny et al., 2009a), the record of atmospheric residual $\Delta^{14}C$ as a proxy for solar activity (Stuiver et al., 1998), the Lake Le Bourget flooding record (Debret et al., 2010) and lake-level highstands in the northwestern Alps (Magny, 2004). Grey horizontal bars indicate periods of increased detrital matter supply in the Lake Iseo sediment record, characterized by abundant turbidites and high magnetic susceptibility. Prior to *c.* 4200 cal. yr BP, there is a close correspondence with intervals of high lake-levels in central-northern Italy and the northwestern Alps, increased detrital flux in Lake Le Bourget and low solar activity, corresponding to wet/cold climate conditions. This indicates a predominant influence of climate variability on detrital matter flux to Lake Iseo. After *c.* 4200 cal. yr BP, detrital input into the lake appears to be controlled by a rather complex interplay between climatic factors (wet/cold conditions) and anthropogenic impact. This is indicated by intervals of high detrital flux occurring during periods of dry/warm climate conditions (high solar activity), which partly overlap with prominent settlement phases

and E_2 are AD 1191±62 (759±62 cal. yr BP) and 355±47 BC (2305±47 cal. yr BP), respectively, while the three smaller event layers E_3, E_4 and E_5 date to 575±62 BC (2525±62 cal. yr BP), 2538±110 BC (4488±110 cal. yr BP) and 6209±173 BC (8159±173 cal. yr BP), respectively (Figure 5).

Discussion

Holocene runoff events and their relation to climate variability and human impact

Frequent small-scale detrital layers in the Lake Iseo sediment record, containing abundant allochthonous minerogenic components and terrestrial plant macrofossils, reflect episodical detrital flux from the catchment. Owing to the clear upward-fining and the occasionally observed erosional basal contacts, the graded detrital layers are interpreted as lacustrine turbidites, deposited by high-density currents acting as underflows (hyperpycnal flows, Mulder and Chapron, 2010; Sturm and Matter, 1978). In contrast, non-graded matrix-supported detrital layers might either reflect successive settling of detrital material from low-density currents acting as inter- or overflows (Chapron et al., 2002; Sturm and Matter, 1978) or represent the distal depositional facies of underflows, entering the lake basin at larger distance from the coring site (Mangili et al., 2005). In any case, the most probable processes for the transport of allochthonous material from the catchment into the lake are either extreme surface runoff events, channelized through subaerial gullies and subaquatic canyons, or propagating terrestrial debris flows and landslides (Hsü and Kelts, 1985; Irmler et al., 2006; Mangili et al., 2005; Sletten et al., 2003) from the hills along the shorelines of the lake. These are all expected to be triggered by exceptionally high precipitation or snowmelt discharge events. The frequent occurrence of mass movements on the SMB slopes throughout the Holocene has also been proven by the seismic survey of Bini et al. (2007), revealing several detrital fans, interpreted as landslide accumulations, along the eastern shoreline. In contrast, river flooding (Bøe et al., 2006; Lambert et al., 1976; Sturm and Matter, 1978) or subaquatic mass flows after the gravitational collapse of slope or delta deposits (Girardclos et al., 2007) are unlikely to cause small-scale detrital layers as (1) there is no major tributary close to the coring site and flood-induced turbidity currents originating from the Oglio River are unlikely to cross the Monte Isola Escarpment (Figure 1) and (2) the frequent occurrence of small-scale detrital layers indicates the absence of long-term sediment storage and thus loading effects on the slopes.

Based on sediment microfacies and magnetic susceptibility data, 12 intervals with increased abundance of small-scale detrital layers and generally increased background flux of detrital matter were identified within the Lake Iseo sediment sequence during the Holocene (Figure 6), revealing a distinct centennial-scale recurrence pattern. These intervals of increased detrital flux occur at *c.* 9800, 9400–8700, 8000–7900, 7600–6900, 6700, 6300–5900, 5700–4900, 4750, 4200–3300, 2950–2700, 2400–1700 and 750–500 cal. yr BP. Although no magnetic susceptibility data are available for the past *c.* 500 years, sediment microfacies inspection revealed two further intervals with several small-scale turbidites, clustering at *c.* 300–200 and 150 cal.

Downloaded from hol.sagepub.com at ETH - Bibliothek on July 26, 2012

yr BP. During the early to mid Holocene, i.e. prior to *c.* 4200 cal. yr BP, periods of increased detrital flux reveal a close correspondence with maxima in atmospheric residual $\Delta^{14}C$ (Stuiver et al., 1998), which are considered to represent periods of low solar activity (Beer, 2000; Muscheler et al., 2000) and in turn are commonly associated with wet/cold climate conditions (Mauquoy et al., 2008; van Geel et al., 1998). These are thought to favour increased catchment erosion through extreme surface runoff events. Hence, intervals of increased detrital matter flux in Lake Iseo during the early Holocene also reveal a good overall agreement with periods of high lake-levels in the northwestern Alps and central Italy (Magny, 2004; Magny et al., 2007) as well as flooding activity in the northwestern Alps (Debret et al., 2010), which are in general also dependent on wet climate conditions. This close agreement between the different proxy records supports the previously supposed significance of Holocene wet-dry cycles over a wide regional scale in the Alpine region (Magny et al., 2007).

After about 4200 cal. yr BP, intervals of increased detrital flux in the Lake Iseo record appear to be partly decoupled from periods of low solar activity (Figure 6) and regional lake-level highstands (Magny, 2004; Magny et al., 2009a), indicating that catchment erosion during the late Holocene might be also controlled by factors other than climate. It has previously been shown that minima in the residual $\Delta^{14}C$ record, reflecting periods of high solar activity and thus dry/warm climate conditions and low lake-levels, were paralleled by increased human impact, e.g. agricultural activity and the construction of lake-dwellings (Magny, 2004; Tinner et al., 2003). In consequence, the apparent occasional correlation between intervals of high solar activity and enhanced detrital matter flux in Lake Iseo during the late Holocene could be related to increased human impact, particularly during climatically favourable dry/warm periods, in the vicinity of the lake since the late Neolithic to early Bronze Age. The first preserved signs of human presence in the Lake Iseo area, namely rock art in the Camonica Valley (Anati, 1994; de Saulieu, 2007), date to the Mesolithic, indicating that the area was already settled prior to *c*. 7000 cal. yr BP. Furthermore, various pollen profiles from the Camonica Valley indicate the onset of agricultural activity in the area at about 7000 cal. yr BP (Gehrig, 1997), a feature consistent with other pollen records along the southern margin of the Alps (Pini, 2002; Tinner et al., 2003). The hypothesis of an onset of significant human influence on detrital flux in Lake Iseo around 4300–4200 cal. yr BP through intensified agricultural activity is supported by a contemporaneous increase in cereal pollen in the Lake Gaiano record, located at the northern margin of Lake Iseo (Gehrig, 1997). Significant increases of cultural indicator plants (e.g. cereals, ruderal plants, grazing indicators) at this time are also observed in other pollen records along the southern margin of the Alps (Pini, 2002; Tinner et al., 2003; Valsecchi et al., 2006). It has previously been shown that human activity (in particular agriculture and forest clearance) strongly affects catchment erosion and thus supply of allochthonous material to a lake (Dapples et al., 2002). Evidence for such an intensification of land use and consequently higher erosional sediment flux to Lake Iseo comes from an increase of sedimentation rate at the onset of the Bronze Age (Figure 6). The absence of an increase in net detrital layer thickness after *c*. 4200 cal. yr BP indicates that the observed late-Holocene sedimentation rate increase must be indeed mainly a reflection of higher background detrital flux, which in turn is most likely related to the increase of human impact at this time.

The first period of presumably mainly human-controlled detrital matter flux comprises the phase of increased agricultural activity during the early to middle Bronze Age and lasted until *c.* 3300 cal. yr BP. The end of this period is contemporaneous with the late Bronze Age decline of cereal pollen in the Lake Gaiano record (Gehrig, 1997), as well as the reduction of indicators for agricultural activity in the nearby Lake Lucone pollen record (Valsecchi et al., 2006) and at other locations in the Southern Alps (Finsinger and Tinner, 2006). This furthermore coincides with the widespread abandonment of lake-dwellings in the Alps around the middle–late Bronze Age transition (Magny, 1993c; Magny et al., 2009b; Tinner et al., 2003), attributed to a shift towards unfavourable wet/cold climate conditions (Magny, 2004). However, the partial coincidence of this interval of high detrital flux with the prominent climate shift around 4200 cal. yr BP (cf. Drysdale et al., 2006; Giraudi et al., 2011; Magny et al., 2009c) highlights the difficulty to disentangle the influences of climate and anthropogenic impact on erosion during this period. The next interval of high detrital matter flux in the Lake Iseo record at *c*. 2950–2700 cal. yr BP broadly corresponds to the late Bronze Age, which is evident as a period of relatively low agricultural activity in the Lake Gaiano (Gehrig, 1997) and Lake Lucone (Valsecchi et al., 2006) pollen records. However, this period incorporates the prominent period of low solar activity and thus wet climate conditions around 2800 cal. yr BP (van Geel et al., 1996), which favoured enhanced flooding and glacier activity in the Alps (Debret et al., 2010; Guyard et al., 2007a). This again indicates the complex interplay between the influences of climate and human impact on erosion processes during the late Holocene in the Lake Iseo area, apparently also valid for the subsequent intervals of increased catchment erosion at 2400–1700 and 750–500 cal. yr BP, which broadly correspond to the Iron Age/early Roman Empire period and the late Middle Ages, respectively. High values of cereal pollen and ruderal plants in the Lake Gaiano record, particularly during the Iron Age and since the late Middle Ages, clearly indicate increased human impact in the Lake Iseo catchment during these intervals (Gehrig, 1997). Furthermore, there is a clear sedimentation rate increase in the Lake Iseo record since the late Middle Ages, which might reflect erosion through intensified land use. Although there is partly also indication for contemporaneous increases of human impact in the pollen records from Lake Lucone (Valsecchi et al., 2006) and Pian di Gembro (Pini, 2002), these intervals partly also incorporate periods of wet/cold climate conditions, e.g. around 1800–1700 and 750–650 cal. yr BP, as revealed from lake-level records (Magny, 2004). The latest periods of increased detrital flux mainly cluster around the Maunder and Dalton solar minima of the 'Little Ice Age'. It therefore could reflect wet/cold climate conditions (cf. Arnaud et al., 2005; Chapron et al., 2002, 2005) as well as increased human impact through rising population density, in particular agricultural activity (cf. Gehrig, 1997) and deforestation for firewood production. However, it is most probably the result of synergetic effects between climatic and anthropogenic influences as seen in other records from mountainous regions (cf. Corella et al., 2011; Morellón et al., 2011).

Pre-historic earthquake activity in the vicinity of Lake Iseo

The five large-scale event layers E_1 to E_5 within the Lake Iseo sediment record reveal a characteristic bipartite structure with basal mass-wasting deposits (slump deposits according to Mulder and Cochonat (1996) and Guyard et al. (2007b)) and overlying large-scale turbidites. Similar deposits have previously been identified in numerous lakes and attributed to past earthquake activity (Bertrand et al., 2008; Blass et al., 2005; Chapron et al., 1999; Fanetti et al., 2008; Moernaut et al., 2007; Monecke et al., 2004; Schnellmann et al., 2002; Siegenthaler et al., 1987). Previous studies have shown that particularly large-scale turbidites may not only have a seismic origin but can also be generated by gravitationally induced sub-aquatic mass flows (Girardclos et al., 2007; Hsü and Kelts, 1985) or extreme surface runoff/flood events (e.g. Bøe et al., 2006; Lambert et al., 1976; Mangili et al., 2005; Sturm and Matter,

Downloaded from hol.sagepub.com at ETH - Bibliothek on July 26, 2012

1978; Sletten et al., 2003). However, in the case of Lake Iseo, a triggering of the large-scale turbidites by strong earthquakes is more likely because (1) the frequent small-scale detrital layers throughout the sediment profile prove the continuous supply of allochthonous material and thus the absence of long-term sediment loading on the slopes and (2) there is no tributary discharging to the SMB and channelized surface flow from extreme rainfall runoff is unlikely to generate hyperpycnal flows of the dimension necessary for the deposition of the two large-scale turbidites within event layers E_1 and E_2 (Mulder and Chapron, 2010).

The hypothesis of a seismic triggering of the five large-scale event layers is further supported by comparison with historical earthquake records in the region. Particularly the strong earthquakes of AD 1117 in Verona and AD 1222 in Brescia with inferred epicentral intensities/magnitudes of I_0=IX–X / M_w=6.5 and I_0=VIII–IX / M_w=6.0, respectively, might have affected the study site. These are considered as the two most destructive historical seismic events in central-northern Italy (Boschi et al., 2000; CPTI Working Group, 2004; Guidoboni et al., 2007) and have been intensively studied by evaluation of historical sources, archaeoseismology and geomorphological evidence (Galadini and Galli, 2001; Galadini et al., 2001; Guidoboni, 1986; Guidoboni et al., 2005; Livio et al., 2009). Macroseismic intensities of these two events in the Lake Iseo area were still in the order of VII to VIII (Guidoboni et al., 2007), although the documentation of local effects attributed to the AD 1117 event is rather ambiguous (Guidoboni et al., 2005; Stucchi et al., 2008). Recent studies have shown that earthquakes exceeding intensities of even VI to VII at the respective site are sufficient to cause liquefaction features within lake sediments (Monecke et al., 2004; Obermeier, 1996), but also landslides, slope failures and seiches (Chapron et al., 1999; Serva, 1994; Siegenthaler et al., 1987) and in consequence large-scale subaquatic mass movements (i.e. slides or slumps), evolving into mass flows and turbidites (Inouchi et al., 1996). The modelled age of AD 1191±62 for large-scale event layer E_1 impedes an unequivocal assignment to either the AD 1117 or the AD 1222 earthquake. However, based on the relationship between earthquake strength, epicentral distance and the generation of large-scale turbidites (Inouchi et al., 1996), we consider large-scale event layer E_1 to be more likely triggered by the adjacent AD 1222 Brescia earthquake (epicentral distance ~25 km) rather than by the more distant AD 1117 Verona earthquake (epicentral distance ~75 km). The second major event layer E_2 is supposed to represent a previously undocumented earthquake around 350 BC. With respect to the spatial pattern and maximum magnitudes/intensities of the historically documented earthquakes in the region (CPTI Working Group, 2004; Guidoboni et al., 2007), the triggering earthquake most probably occurred within a radius of about 30–40 km and reached a magnitude and intensity of M_w=5.0–6.5 and I_0=VII–IX, respectively. An explanation for the different sediment facies of the basal mass-wasting deposits of both large-scale event layers could be a different distance of the initial slope failure, resulting in a proximal-distal pattern as observed for turbidites, debris flows and slump-generated deposits in Lake Zurich (Hsü and Kelts, 1985).

The three large-scale event layers E_3, E_4 and E_5 in the lower part of the sediment sequence, dating to 575±62 BC, 2538±110 BC and 6209±173 BC, respectively, are relatively thin compared with event layers E_1 and E_2. However, because of their similar bipartite structure they are supposed to also reflect previously undocumented pre-historic earthquakes with magnitudes of at least M_W=5.0. The reduced thickness of these event layers indicates, however, not necessarily that the triggering earthquakes were significantly smaller than those causing event layers E_1 and E_2. A possible cause for the reduced thickness of event layers E_3–E_5 could be the generally lower background supply of detrital material during the early Holocene. Enhanced detrital matter flux due to the increased human activity in the catchment since the Bronze Age might have increased the amount of sediment available for mobilization through slope failures induced by the earthquakes of AD1222 and 350 BC. Another explanation for the variable thickness of the large-scale event layers might be site effects, e.g. more distal initial slope failures for the event layers E_3, E_4 and E_5 than for the two larger event layers. Besides the complex relationship between earthquake intensity, epicentral distance and the generation of slope failures, this could also explain the lacking evidence for other proximal earthquakes like those in Sarnico and Montecchio (Table 1), which should have also produced slope failures, but possibly only in the southern basin of Lake Iseo. In consequence, the Lake Iseo palaeoseismic record must be considered as incomplete but nevertheless, it provides valuable insights into local seismic activity prior to the documentary period, which might be confirmed and extended by the investigation of other regional lake sediment records.

Conclusions

- Prior to *c.* 4200 cal. yr BP, the occurrence of small-scale turbidites and intervals of generally increased detrital matter flux in the Lake Iseo sediment record reveals a close correspondence with periods of low solar activity, increased flooding in large alpine rivers and regional lake-level highstands, reflecting wet and cold climate conditions. This indicates that catchment erosion during the early to mid Holocene was mainly driven by natural climate variability.
- With the increase of human impact in the vicinity of the lake after *c.* 4200 cal. yr BP, intervals of increased occurrence of small-scale turbidites and detrital matter flux and thus enhanced catchment erosion appear to be partly decoupled from climatic fluctuations (wet and cold climate conditions) and also influenced to a certain degree by anthropogenic land use activity.
- Five large-scale event layers composed of basal mass-wasting deposits and overlying turbidites were identified within the profile, which are attributed to major regional earthquakes. Radiocarbon dating provides evidence for a correlation of the uppermost event layer with a documented M_w=6.0 earthquake in AD 1222 in Brescia. The four older large-scale event layers are supposed to be related to previously undocumented earthquakes, which occurred prior to the period covered by regional earthquake catalogues around 350 BC, 570 BC, 2540 BC and 6210 BCand most probably also exceeded M_w=5.0.

Acknowledgements

We are indebt to the owners of the Riva di San Pietro camping site for facilitating the field lab. Gabriele Arnold, Dieter Berger and Michael Köhler (GFZ Potsdam) are acknowledged for preparing high-quality thin sections and Brian Brademann (GFZ Potsdam) for assisting microscopic thin section analysis. Maxime Debret (Université de Rouen) kindly provided the Lake Le Bourget data. The valuable comments of two anonymous reviewers helped to improve an earlier version of the manuscript. The Lake Iseo data presented in this study are available at doi: 10.5880/GFZ.2011.100 and via the PANGAEA network.

Funding

This study is part of the DecLakes project within the frame of the European Science Foundation EUROCORES Programme EuroCLIMATE (contract No. ERAS-CT-2003-980409 of the European Commission, DG Research, FP6, ESF project DecLakes no. 04-ECLIM-FP29) and has been funded by the national

Downloaded from hol.sagepub.com at ETH - Bibliothek on July 26, 2012

agencies DFG (Germany, project no. BR2208/2-2, AN554/1-2), CNRS (France) and MEC (Spain, project no. CGL2005-23766-E/CLI).

References

Anati E (1994) *Valcamonica Rock Art – A New History for Europe*. Capo di Ponte: Centro Camuno di Studi Preistorici.

Arbogast R-M, Jacomet S, Magny M et al. (2006) The significance of climate fluctuations for lake level changes and shifts in subsistence economy during the late Neolithic (4300–2400 B.C.) in central Europe. *Vegetation History and Archaeobotany* 15: 403–418.

Arnaud F, Revel M, Chapron E et al. (2005) 7200 years of Rhone river flooding activity in Lake Le Bourget, France: A high-resolution sediment record of NW Alps hydrology. *The Holocene* 15: 420–428.

Beer J (2000) Long-term indirect indices of solar variability. *Space Science Reviews* 94: 53–66.

Bertrand S, Charlet F, Chapron E et al. (2008) Reconstruction of the Holocene seismotectonic activity of the Southern Andes from seismites recorded in Lago Icalma, Chile, 39°S. *Palaeogeography Palaeoclimatology Palaeoecology* 259: 301–322.

Bini A, Cita MB and Gaetani M (1978) Southern Alpine lakes: Hypothesis of an erosional origin related to the Messinian entrenchment. *Marine Geology* 27: 271–288.

Bini A, Cobari D, Falletti P et al. (2007) Morphology and geological setting of Iseo Lake (Lombardy) through multibeam bathymetry and high-resolution seismic profiles. *Eclogae Geologicae Helvetiae* 100: 23–40.

Blass A, Anselmetti FS, Grosjean M et al. (2005) The last 1300 years of environmental history recorded in the sediments of Lake Sils (Engadine, Switzerland). *Eclogae Geologicae Helvetiae* 98: 319–332.

Bøe A-G, Dahl SO, Lie Ø et al. (2006) Holocene river floods in the upper Glomma catchment, southern Norway: A high-resolution multiproxy record from lacustrine sediments. *The Holocene* 16: 445–455.

Boschi E, Guidoboni E, Ferrari G et al. (2000) Catalogue of strong Italian earthquakes from 461 B.C. to 1997. *Annali di Geofisica* 43: 609–868.

Bradshaw R and Thompson R (1985) The use of magnetic measurements to investigate the mineralogy of Icelandic lake sediments and to study catchment processes. *Boreas* 14: 203–215.

Brauer A and Casanova J (2001) Chronology and depositional processes of the laminated sediment record from Lac d'Annecy, French Alps. *Journal of Paleolimnology* 25: 163–177.

Brauer A, Endres C and Negendank JFW (1999) Lateglacial calendar year chronology based on annually laminated sediments from Lake Meerfelder Maar, Germany. *Quaternary International* 61: 17–25.

Burrato P, Ciucci F and Valensise G (2003) An inventory of river anomalies in the Po Plain, Northern Italy: Evidence for active blind thrust faulting. *Annals of Geophysics* 46: 865–882.

Cassinis G, Corbari D, Falletti P et al. (2009) *Note illustrative della carta geologica d'Italia alla scala 1: 50.000. Foglio 99 Iseo*. Roma: APAT, Servizio Geologico d'Italia.

Castellarin A and Cantelli L (2000) Neo-Alpine evolution of the southern Eastern Alps. *Journal of Geodynamics* 30: 251–274.

Castellarin A, Vai GB and Cantelli L (2006) The Alpine evolution of the Southern Alps around the Giudicarie faults: A Late Cretaceous to Early Eocene transfer zone. *Tectonophysics* 414: 203–223.

Chapman MR and Shackleton NJ (1998) What level of resolution is attainable in a deep-sea core? Results of a spectrophotometer study. *Paleoceanography* 13: 311–315.

Chapron E, Arnaud F, Noël H et al. (2005) Rhone River flood deposits in Lake Le Bourget: A proxy for Holocene environmental changes in the NW Alps, France. *Boreas* 34: 404–416.

Chapron E, Beck C, Pourchet M et al. (1999) 1822 earthquake-triggered homogenite in Lake Le Bourget (NW Alps). *Terra Nova* 11: 86–92.

Chapron E, Desmet M, de Putter T et al. (2002) Climatic variability in the northwestern Alps, France, as evidenced by 600 years of terrigenous sedimentation in Lake Le Bourget. *The Holocene* 12: 177–185.

Chunga K, Livio F, Michetti AM et al. (2007) Synsedimentary deformation of Pleistocene glaciolacustrine deposits in the Albese con Cassano Area (Southern Alps, Northern Italy), and possible implications for paleoseismicity. *Sedimentary Geology* 196: 59–80.

Corella JP, Moreno A, Morellón M et al. (2011) Climate and human impact on a meromictic lake during the last 6,000 years (Montcortès Lake, Central Pyrenees, Spain). *Journal of Paleolimnology* 46: 351–367.

CPTI Working Group (2004) *Catalogo Parametrico dei Terremoti Italiani 2004 (CPTI04)*. Bologna (http://emidius.mi.ingv.it/CPTI/): INGV.

Dal Piaz GV, Bistacchi A and Massironi M (2003) Geological outline of the Alps. *Episodes* 26: 175–180.

Dapples F, Lotter AF, van Leeuwen JFN et al. (2002) Paleolimnological evidence for increased landslide activity due to forest clearing and land-use since 3600 cal BP in the western Swiss Alps. *Journal of Paleolimnology* 27: 239–248.

de Saulieu G (2007) Gravures rupestres et statues-menhirs alpines du Chalcolithique à l'Âge du Bronze moyen: Reflets de processus sociaux. In: Richard H, Magny M and Mordant C (eds) *Environnements et cultures à l'Âge du Bronze en Europe occidentale*. Éditions du CTHS, 357–374.

Debret M, Chapron E, Desmet M et al. (2010) North western Alps Holocene paleohydrology recorded by flooding activity in Lake Le Bourget, France. *Quaternary Science Reviews* 29: 2185–2200.

Drysdale R, Zanchetta G, Hellstrom J et al. (2006) Late Holocene drought responsible for the collapse of Old World civilizations is recorded in an Italian cave flowstone. *Geology* 34: 101–104.

Fanetti D, Anselmetti FS, Chapron E et al. (2008) Megaturbidite deposits in the Holocene basin fill of Lake Como (southern Alps, Italy). *Palaeogeography, Palaeoclimatology, Palaeoecology* 259: 323–340.

Fantoni R, Bersezio R and Forcella F (2004) Alpine structure and deformation chronology at the southern Alps-Po Plain border in Lombardy. *Bollettino della Società Geologica Italiana* 123: 463–476.

Finsinger W and Tinner W (2006) Holocene vegetation and land-use changes in response to climatic changes in the forelands of the southwestern Alps, Italy. *Journal of Quaternary Science* 21: 243–258.

Galadini F and Galli P (2001) Archaeoseismology in Italy: Case studies and implications on long-term seismicity. *Journal of Earthquake Engineering* 5: 35–68.

Galadini F, Galli P, Molin D et al. (2001) Searching for the source of the 1117 earthquake in Northern Italy: A multidisciplinary approach. In: Glade T, Albini P and Francés F (eds) *The Use of Historical Data in Natural Hazard Assessments*. Kluwer Academic Publishers, 3–27.

Garibaldi L, Mezzanotte V, Brizzio MC et al. (1999) The trophic evolution of Lake Iseo as related to its holomixis. *Journal of Limnology* 58: 10–19.

Gehrig R (1997) Pollenanalytische Untersuchungen zur Vegetations- und Klimageschichte des Val Camonica (Norditalien). *Dissertationes Botanicæ* 276: 1–152.

Girardclos S, Schmidt OT, Sturm M et al. (2007) The 1996 AD delta collapse and large turbidite in Lake Brienz. *Marine Geology* 241: 137–154.

Giraudi C, Magny M, Zanchetta G et al. (2011) The Holocene climatic evolution of Mediterranean Italy: A review of the continental geological data. *The Holocene* 21: 105–115.

Guidoboni E (1986) The earthquake of December 25, 1222: Analysis of a myth. *Geologia Applicata e Idrogeologia* 21: 413–424.

Guidoboni E, Comastri A and Boschi E (2005) The 'exceptional' earthquake of 3 January 1117 in the Verona area (northern Italy): A critical time review and detection of two lost earthquakes (lower Germany and Tuscany). *Journal of Geophysical Research* 110: B12309.

Guidoboni E, Ferrari G, Mariotti D et al. (2007) CFTI4Med – Catalogue of strong earthquakes in Italy (461 B.C.–1997) and Mediterranean area (760 B.C.–1500). INGV-SGA, accessible at http://storing.ingv.it/cfti4med/.

Guyard H, Chapron E, St-Onge G et al. (2007a) High-altitude varve records of abrupt environmental changes and mining activity over the last 4000 years in the Western French Alps (Lake Bramant, Grandes Rousses Massif). *Quaternary Science Reviews* 26: 2644–2660.

Guyard H, St-Onge G, Chapron E et al. (2007b) The AD 1881 earthquake-triggered slump and late Holocene flood-induced turbidites from proglacial Lake Bramant, western French Alps. In: Lykousis V, Sakellariou D and Locat J (eds) *Submarine Mass Movements and Their Consequences*. Advances in Natural and Technological Hazards Research 27, pp. 279–286.

Hsü KJ and Kelts K (1985) Swiss lakes as a geological laboratory. Part I: Turbidity currents. *Naturwissenschaften* 72: 315–321.

Inouchi Y, Kinugasa Y, Kumon F et al. (1996) Turbidites as records of intense palaeoearthquakes in Lake Biwa, Japan. *Sedimentary Geology* 104: 117–125.

Irmler R, Daut G and Mäusbacher R (2006) A debris flow calendar derived from sediments of lake Lago di Braies (N. Italy). *Geomorphology* 77: 69–78.

Lambert AM, Kelts K and Marshall NF (1976) Measurements of density underflows from Walensee, Switzerland. *Sedimentology* 23: 87–105.

Livio FA, Berlusconi A, Michetti AM et al. (2009) Active fault-related folding in the epicentral area of the December 25, 1222 (I_0 = IX MCS) Brescia earthquake (Northern Italy): Seismotectonic implications. *Tectonophysics* 476: 320–335.

Magny M (1993a) Holocene fluctuations of lake levels in the French Jura and sub-Alpine ranges, and their implications for past general circulation patterns. *The Holocene* 3: 306–313.

Magny M (1993b) Solar influences on Holocene climatic changes illustrated by correlations between past lake-level fluctuations and the atmospheric ^{14}C record. *Quaternary Research* 40: 1–9.

Downloaded from hol.sagepub.com at ETH - Bibliothek on July 26, 2012

Magny M (1993c) Un cadre climatique pour les habitats lacustres préhistoriques? *Comptes Rendus de l'Academie des Sciences* 316: 1619–1625.

Magny M (2004) Holocene climate variability as reflected by mid-European lake-level fluctuations and its probable impact on prehistoric human settlements. *Quaternary International* 113: 65–79.

Magny M, Arnaud F, Holzhauser H et al. (2010) Solar and proxy-sensitivity imprints on paleohydrological records for the last millennium in west-central Europe. *Quaternary Research* 73: 173–179.

Magny M, de Beaulieu JL, Drescher-Schneider R et al. (2007) Holocene climate changes in the central Mediterranean as recorded by lake-level fluctuations at Lake Accesa (Tuscany, Italy). *Quaternary Science Reviews* 26: 1736–1758.

Magny M, Galop D, Bellintani P et al. (2009a) Late-Holocene climatic variability south of the Alps as recorded by lake-level fluctuations at Lake Ledro, Trentino, Italy. *The Holocene* 19: 575–589.

Magny M, Peyron O, Gauthier E et al. (2009b) Quantitative reconstruction of climatic variations during the Bronze and early Iron ages based on pollen and lake-level data in the NW Alps, France. *Quaternary International* 200: 102–110.

Magny M, Vanniere B, Zanchetta G et al. (2009c) Possible complexity of the climatic event around 4300–3800 cal. BP in the central and western Mediterranean. *The Holocene* 19: 823–833.

Mangili C, Brauer A, Moscariello A et al. (2005) Microfacies of detrital event layers deposited in Quaternary varved lake sediments of the Piànico-Sèllere Basin (northern Italy). *Sedimentology* 52: 927–943.

Mauquoy D, Yeloff D, Van Geel B et al. (2008) Two decadally resolved records from north-west European peat bogs show rapid climate changes associated with solar variability during the mid-late Holocene. *Journal of Quaternary Science* 23: 745–763.

Migowski C, Agnon A, Bookman R et al. (2004) Recurrence pattern of Holocene earthquakes along the Dead Sea transform revealed by varve-counting and radiocarbon dating of lacustrine sediments. *Earth and Planetary Science Letters* 222: 301–314.

Moernaut J, De Batist M, Charlet F et al. (2007) Giant earthquakes in South-Central Chile revealed by Holocene mass-wasting events in Lake Puyehue. *Sedimentary Geology* 195: 239–256.

Monecke K, Anselmetti FS, Becker A et al. (2004) The record of historic earthquakes in lake sediments of central Switzerland. *Tectonophysics* 394: 21–40.

Morellón M, Valero-Garcés B, González-Sampériz P et al. (2011) Climate changes and human activities recorded in the sediments of Lake Estanya (NE Spain) during the Medieval Warm Period and Little Ice Age. *Journal of Paleolimnology* 46: 423–452.

Moreno A, Valero-Garcés B, González-Sampériz P et al. (2008) Flood response to rainfall variability during the last 2000 years inferred from the Taravilla Lake record (Central Iberian Range, Spain). *Journal of Paleolimnology* 40: 943–961.

Mulder T and Chapron E (2010) Flood deposits in continental and marine environments: Character and significance. In: Slatt RM and Zavala C (eds) *Sediment Transfer from Shelf to Deep Water – Revisiting the Delivery System*. AAPG Studies in Geology 61, pp. 1–30.

Mulder T and Cochonat P (1996) Classification of offshore mass movements. *Journal of Sedimentary Research* 66: 43–57.

Muscheler R, Beer J, Wagner G et al. (2000) Changes in deep-water formation during the Younger Dryas event inferred from ^{10}Be and ^{14}C records. *Nature* 408: 567–570.

Nomade J, Chapron E, Desmet M et al. (2005) Reconstructing historical seismicity from lake sediments (Lake Laffrey, Western Alps, France). *Terra Nova* 17: 350–357.

Obermeier SF (1996) Use of liquefaction-induced features for paleoseismic analysis – An overview of how seismic liquefaction features can be distinguished from other features and how their regional distribution and properties of source sediment can be used to infer the location and strength of Holocene paleo-earthquakes. *Engineering Geology* 44: 1–76.

Pini R (2002) A high-resolution Late-Glacial–Holocene pollen diagram from Pian di Gembro (Central Alps, Northern Italy). *Vegetation History and Archaeobotany* 11: 251–262.

Ramsey CB (1995) Radiocarbon calibration and analysis of stratigraphy: the OxCal program. *Radiocarbon* 37: 425–430.

Ramsey CB (2001) Development of the radiocarbon calibration program. *Radiocarbon* 43: 355–363.

Ramsey CB (2008) Deposition models for chronological records. *Quaternary Science Reviews* 27: 42–60.

Reimer PJ, Baillie MGL, Bard E et al. (2009) IntCal09 and Marine09 radiocarbon age calibration curves, 0-50,000 years cal BP. *Radiocarbon* 51: 1111–1150.

Schneider H, Höfer D, Irmler R et al. (2010) Correlation between climate, man and debris flow events – A palynological approach. *Geomorphology* 120: 48–55.

Schnellmann M, Anselmetti FS, Giardini D et al. (2002) Prehistoric earthquake history revealed by lacustrine slump deposits. *Geology* 30: 1131–1134.

Serpelloni E, Anzidei M, Baldi P et al. (2005) Crustal velocity and strain-rate fields in Italy and surrounding regions: New results from the analysis of permanent and non-permanent GPS networks. *Geophysical Journal International* 161: 861–880.

Serva L (1994) Ground effects in intensity scales. *Terra Nova* 6: 414–416.

Siegenthaler C, Finger W, Kelts K et al. (1987) Earthquake and seiche deposits in Lake Lucerne, Switzerland. *Eclogae Geologicae Helvetiae* 80: 241–260.

Sileo G, Michetti AM, Chunga K et al. (2007) Remarks on the Quaternary tectonics of the Insubria Region (Lombardia, NW Italy, and Ticino, SE Switzerland). *Bollettino della Società Geologica Italiana* 126: 411–425.

Sletten K, Blikra LH, Ballantyne CK et al. (2003) Holocene debris flows recognized in a lacustrine sedimentary succession: Sedimentology, chronostratigraphy and cause of triggering. *The Holocene* 13: 907–920.

Strasser M, Anselmetti FS, Faeh D et al. (2006) Magnitudes and source areas of large prehistoric northern Alpine earthquakes revealed by slope failures in lakes. *Geology* 34: 1005–1008.

Stucchi M, Galadini F, Rovida A et al. (2008) Investigation of pre-1700 earthquakes between the Adda and the middle Adige River basins (Southern Alps). In: Fréchet J, Meghraoui M and Stucchi M (eds) *Historical Seismology*. Springer, 93–129.

Stuiver M, Reimer PJ, Bard E et al. (1998) INTCAL98 radiocarbon age calibration, 24,000–0 cal BP. *Radiocarbon* 40: 1041–1083.

Sturm M and Matter A (1978) Turbidites and varves in Lake Brienz (Switzerland): Deposition of clastic detritus by density currents. In: Matter A and Tucker ME (eds) *Modern and Ancient Lake Sediments*. Blackwell, Special Publication of the International Association of Sedimentologists 2, pp. 147–168.

Thompson R, Battarbee RW, O'Sullivan PE et al. (1975) Magnetic susceptibility of lake sediments. *Limnology and Oceanography* 20: 687–698.

Tinner W, Lotter AF, Ammann B et al. (2003) Climatic change and contemporaneous land-use phases north and south of the Alps 2300 BC to 800 AD. *Quaternary Science Reviews* 22: 1447–1460.

Valsecchi V, Tinner W, Finsinger W et al. (2006) Human impact during the Bronze Age on the vegetation at Lago Lucone (northern Italy). *Vegetation History and Archaeobotany* 15: 99–113.

van Geel B, Buurman J and Waterbolk HT (1996) Archaeological and palaeoecological indications of an abrupt climate change in the Netherlands, and evidence for climatological teleconnections around 2650 BP. *Journal of Quaternary Science* 11: 451–460.

van Geel B, van der Plicht J, Kilian MR et al. (1998) The sharp rise of Δ^{14}C ca. 800 cal BC: Possible causes, related climatic teleconnections and the impact on human environments. *Radiocarbon* 40: 535–550.

Vose RS, Schmoyer RL, Steurer PM et al. (1992) *The Global Historical Climatology Network: Long-term Monthly Temperature, Precipitation, Sea Level Pressure, and Station Pressure Data*. ORNL/CDIAC-53, NDP-041. Oak Ridge, Tennessee: Carbon Dioxide Information Analysis Center, Oak Ridge National Laboratory.

Downloaded from hol.sagepub.com at ETH - Bibliothek on July 26, 2012